First flights of a new airborne thermal infrared imaging spectrometer with high area coverage

Jeffrey L. Hall*, Richard H. Boucher, David J. Gutierrez, Steven J. Hansel,
Brian P. Kasper, Eric R. Keim, Nery M. Moreno, Mark L. Polak,
Mazaher G. Sivjee, David M. Tratt, David W. Warren
The Aerospace Corporation, P.O. Box 92957, Los Angeles, CA, USA 90009-2957

ABSTRACT

A new airborne thermal infrared imaging spectrometer, "Mako", with 128 bands in the thermal infrared covering 7.8 to 13.4 microns, has recently completed its engineering flight trials. Results from these flights, which occurred in September 2010 and included two science flights, are presented. The new sensor flies in a Twin Otter aircraft and operates in a whiskbroom mode, giving it the ability to scan to ±40° around nadir. The sensor package is supported on a commercial 3-axis-stabilized mount which greatly reduces aircraft-induced pointing jitter. The internal optics and focal plane array are operated near liquid helium temperatures, which in conjunction with a fast f/1.25 spectrometer enables low noise performance despite the sensor's small (0.55 mrad) pixel size and the high frame rate needed to cover large whisk angles. Besides the large-area-coverage scan mode (20 km^2 per minute at 2-meter GSD from 12,500 ft. AGL), the sensor features a scan mirror pitch capability that enables both a high-sensitivity mode (longer integration times using frame summing, covering a smaller spatial region) and a multiple-look mode (multiple looks at a smaller region in a single aircraft overpass, for discriminating plume motion, for example).

Keywords: high area coverage, infrared imaging spectrometer, airborne sensor, Dyson spectrometer, hyperspectral

1. INTRODUCTION

The availability of sensitive, high-frame-rate focal plane arrays in the thermal infrared coupled with advances in the design of low-distortion, optically-fast spectrometers based on a Dyson prescription has enabled construction of a new airborne spectral imaging sensor, "Mako", with comparable sensitivity but much larger area coverage rate compared to previous sensors. In this new sensor the pitch (along-track) angle of the scan mirror is also controllable, permitting two new modes of operation: a staring mode, in which multiple frames of data are coadded to increase sensitivity, and a multiple-look mode, in which multiple whisks of the same area can be completed in a single aircraft overpass. These latter modes necessarily scan over smaller whisk angles than for the large-area-coverage mode.

2. THE MAKO SENSOR

The Mako airborne sensor, a follow-on to our SEBASS[1] sensor, has been described in detail elsewhere[2]; here we will highlight the major features of the instrument. It uses a 128×128 Si:As blocked impurity band focal plane array (FPA) manufactured by DRS Technologies. It is operated at 10K using LHe cryogen and has an operability of 99.93%. The optics are also cooled to near-LHe temperatures. The spectrometer has an entrance slit which is imaged onto one axis of the detector array while the other axis is used for spectral dispersion, which is achieved using a concave grating in conjunction with a Dyson lens. The Dyson design permits operation at fast f-numbers (Mako operates at f/1.25) while keeping "smile" and "keystone" distortions low. The Dyson prescription is modified by adding a "corrector" lens that provides sufficient relief from the rear surface of the Dyson lens to mount the FPA and slit assemblies. The spectral resolution of the sensor, as determined from measurements of calibration films, is comparable to its spectral sampling, which is 0.044 μm (equivalent to ~4 cm^{-1} at 10 μm).

The pupil image at the cold stop within the sensor dewar has a diameter of 30 mm, and a three-mirror afocal telescope external to the dewar reduces the pixel IFOV by a factor of 3.7 and results in an entrance pupil diameter of 4.3 inches. The pixel IFOV is 550 microradians, and the scan mirror whisk speed is adjusted to produce approximately square pixels

*jeffrey.l.hall@aero.org; phone 1 310 336-7615; fax 1 310 563-2528; www.aero.org

Infrared Technology and Applications XXXVII, edited by Bjørn F. Andresen, Gabor F. Fulop, Paul R. Norton,
Proc. of SPIE Vol. 8012, 801203 · © 2011 SPIE · CCC code: 0277-786X/11/$18 · doi: 10.1117/12.884865

at nadir. Figure 1 indicates the major components of Mako, and Figure 2 shows the sensor installed in a Twin Otter International DeHavilland DHC-6 Twin Otter aircraft. The whole sensor assembly sits on a 3-axis, gyro-stabilized mount that greatly reduces both low- and high-frequency pointing jitter due to aircraft motions and propeller-induced vibration. The gimbal mirror directs the line-of-sight of the instrument through an open rectangular port in the bottom of the fuselage. The image of the sensor slit is aligned parallel to the direction of travel of the aircraft. The cross-track whisking of the slit image to the left and right of the aircraft is done with a gimbal mirror controlled by a servo motor, and a separate pitch motor enables the additional scan modes described above by compensating for the forward motion of the airplane.

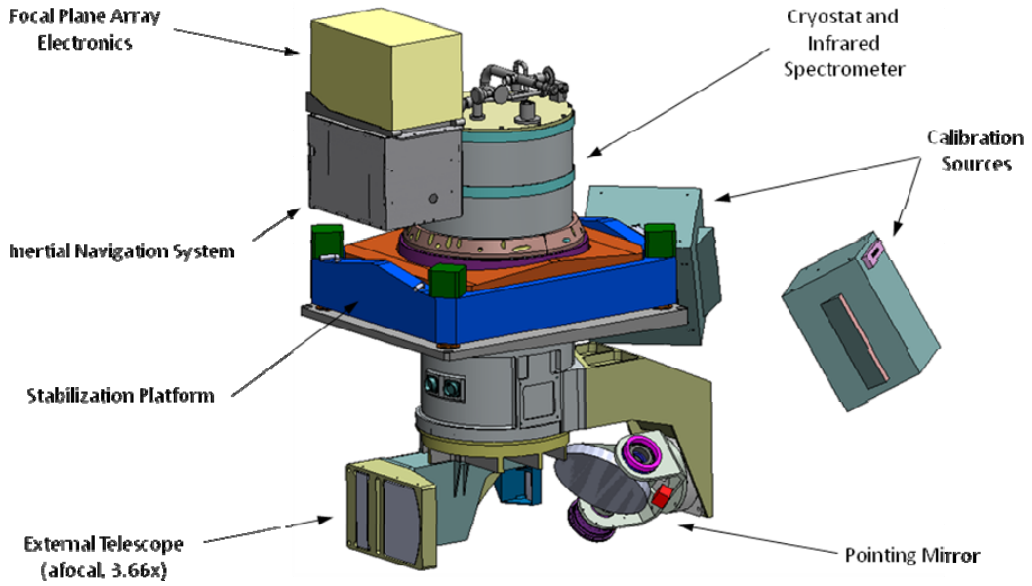

Figure 1. Major components of the Mako sensor. The 3-axis stabilization platform (Intergraph Z/I mount), inertial navigation system (Litton LN100-G) and calibration sources (SBIR Inc. DDB-06) are all COTS devices. The stabilization platform base and calibration sources are affixed to a heavy duty frame (not shown) that is in turn anchored to the Douglas track in the Twin Otter aircraft.

Figure 2. Mako sensor installed in the rear of a Twin Otter aircraft, where it looks down through a rectangular port in the bottom of the fuselage.

3. SENSOR PERFORMANCE

Engineering flights were conducted over the course of eight days in September 2010 and were supplemented by two days of science flights. The installation of the sensor package into the Twin Otter aircraft was accomplished in less than 3 hours. The dewar hold time of more than 36 hours meant that a single daily fill of cryogen was sufficient to keep the sensor cold throughout the test period. The test flights were conducted at altitudes as low as 3000 ft. AGL and as high as 12,500 ft. MSL. The latter altitude is the highest that can be flown without the need for oxygen by the crew.

The DRS FPA has 16 output taps and is capable of running at up to a 4 kHz frame rate. For Mako our initial goal was to run the array at 2 kHz, which would enable almost full-width (±40°) whisks even at an aircraft altitude of only 3000 ft. AGL. In this first incarnation of the sensor the A/D board that digitized the detector signals was physically located some distance from the sensor dewar, resulting in significant cable capacitance that limited frame rates to 800 Hz. This in turn required decreasing the integration time to 30% of the frame period to prevent saturation at higher scene temperatures. As a result, the current NEDT of the sensor is higher than the design goal. It was measured in the lab as 0.1°C at 10 microns and 298K for a single frame. (The NEDT is nominally constant towards the 13 micron end of the spectral range, but increases to almost 0.2°C at the 7.5 micron end.) An almost identical NEDT curve was measured during the sensor flights. The sensor noise measured in the lab exhibited the expected $N^{-1/2}$ noise reduction upon frame coadding (up to 32 frames), although similar performance behavior was not achievable aboard the aircraft. Rectification of these deficiencies is currently underway.

All of the sensor scan modes were tested during the engineering flights. For large-area scanning datasets were acquired covering slightly more than ±40° around nadir and consisting of 100 contiguous whisks along the flight path, which required almost 8 minutes. Figure 3 shows a screen shot of the thermal image of one of those datasets. This scan configuration gives an area scan rate of 20 km^2 per minute from an altitude of 12,500 ft. AGL at a pixel resolution of 2 meters (compared to 0.8 km^2 per minute for SEBASS at the same spatial resolution). Calibration data, obtained by separately pointing the gimbal mirror at two temperature-controlled flat plate blackbody sources, is acquired immediately before and after each set of whisks. The sensor can theoretically acquire an unlimited number of contiguous whisks (subject only to storage volume); however, sensor calibration drift dictates the 100-whisk maximum we have tested.

Figure 3. Screen shot showing the center two-thirds of 6 whisks excerpted from a 100-whisk Mako dataset acquired over an urban area in Los Angeles. The aircraft flight path is from bottom to top of this view, roughly along the center, and the Mako gimbal mirror slews to the left and right of nadir. Each whisk consists of 128 vertical pixels. In this dataset each whisk contains 2800 frames of data (horizontal pixels, corresponding to slightly more than ± 40° around nadir), for a total of 358,400 pixels per whisk. Each pixel has a 128-channel spectrum associated with it. This data was acquired at 12,500 ft. AGL, at which altitude the pixel size is ~ 2 meters. The picture also clearly shows the overlap between whisks, which is a programmable quantity with a default value of 10%.

The ability to control the pitch of the gimbal mirror has enabled two new modes for the sensor besides the "high sensitivity" (staring) mode originally envisioned. The first is bi-directional whisking, in which the gimbal mirror pitch is controlled to compensate for the forward motion of the aircraft and which is employed to create whisks that are almost perpendicular to the aircraft motion. This increases the effective duty cycle for the scan patterns, thereby permitting larger angle scans at lower aircraft altitudes. The second capability is the ability to scan the same limited-area scene more than once in a single aircraft overpass. This mode was also successfully demonstrated during the engineering flights. This mode is useful for measuring chemical plume motion, for example.

We have examined the geolocation accuracy of our data using the Central Valley dataset described below. For a couple of datasets we have compared measured latitude and longitude data from up to 10 points per whisk of prominent building corners, road intersections etc. with coordinates extracted from Google Earth. We demonstrated the accuracy of the Google Earth data in this region during an earlier excursion to in the area with a truck outfitted with a differential GPS set-up. That data had shown 1-2 meter agreement between the truck GPS and the corresponding Google Earth coordinates. Initial Mako results showed agreement within 5-10 meters, independent of whisk angle, whisk number, or aircraft heading. A more comprehensive analysis of these errors is in progress.

4. SCIENCE FLIGHTS

4.1 California Central Valley

California's Central Valley is an area of intensive dairy and arable agriculture that is a principal source of atmospheric ammonia for the region. A recent paper[3] describes ammonia detections acquired over the area by the IASI (Infrared Atmospheric Sounding Interferometer) satellite sensor. IASI is a high-spectral-resolution infrared atmospheric sounding sensor in a sun-synchronous low-earth orbit that scans every point on the Earth at least twice per day (daytime crossing time is 9:30 a.m. local at the equator). The IASI measurements indicated large concentrations of ammonia over many areas of the Central Valley. A truck-mounted FTIR remote sensor was deployed to the area to verify that the ammonia signals would be observable with our Mako airborne sensor. The FTIR sensor was pointed at zenith and took data continuously as the truck traversed many roads in the agricultural regions of Tulare County. The levels of ammonia measured with this FTIR reached 100 ppm-meters in some locations, providing confidence that Mako would successfully detect the ambient ammonia concentrations present.

Morning and afternoon flights were conducted over the Central Valley in Tulare County, the former to coincide with overpasses of IASI. Figure 4 shows a brightness temperature image of one of the whisk sets acquired in the afternoon. In this figure overlapping data from adjacent whisks has been removed. The data clearly shows the location of the dairy farms, and the agricultural fields are relatively cool if they are vegetated (plants or trees), and considerably warmer if they are barren (such as freshly ploughed fields or in the vicinity of the dairy operations). Figure 5 shows the ammonia column density map that was derived from the Mako spectral measurements recorded with each pixel.

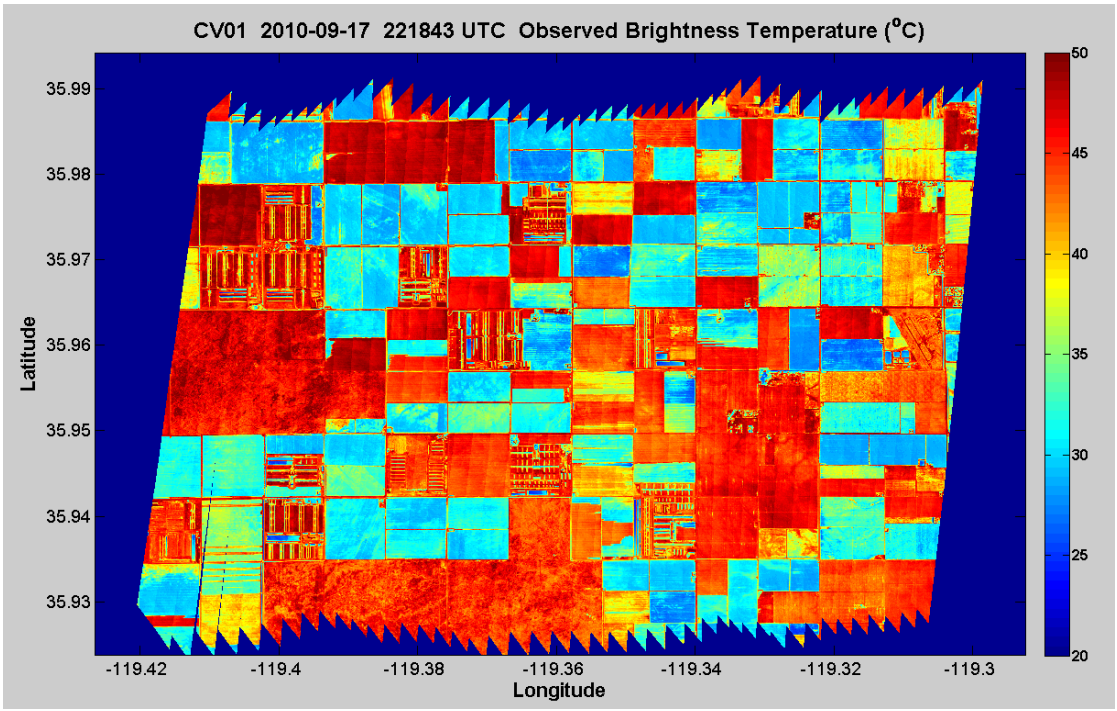

Figure 4. Brightness temperature map at 10.7 μm (in °C) of an 11 × 6.5 km region (45-whisk dataset) near Pixley in Tulare County, California. Data were acquired from an aircraft altitude of 12,500 ft AGL. Aircraft motion is from left to right. The dairy farms are the squares that contain the elongated rectangles.

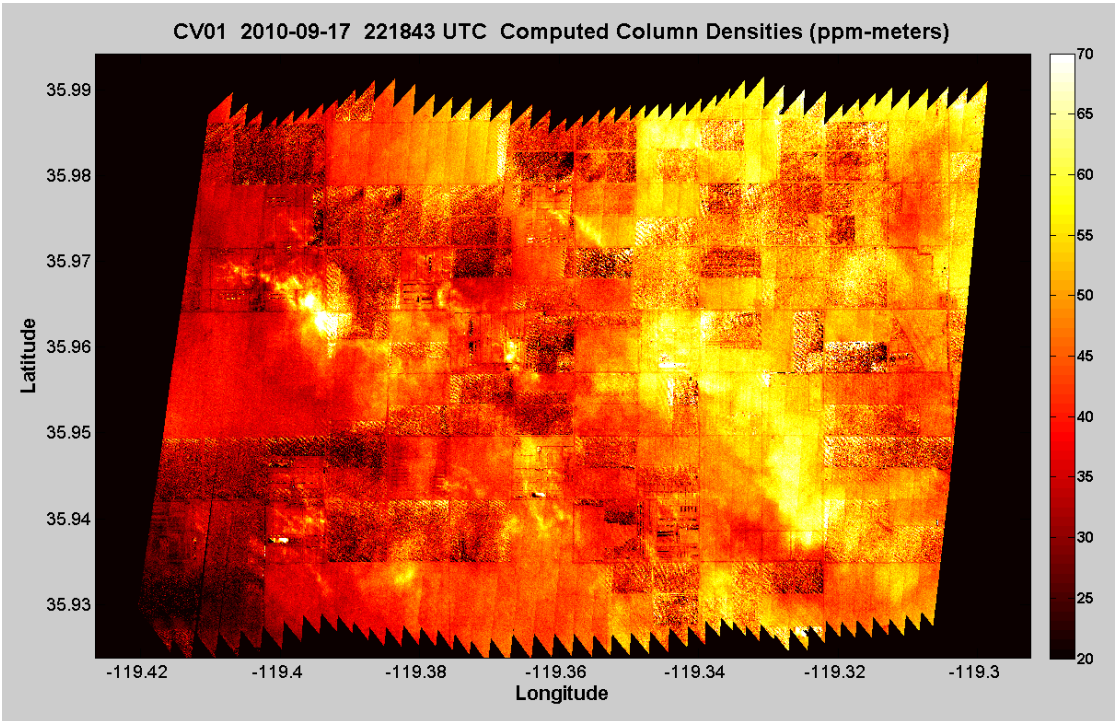

Figure 5. Retrieved ammonia column densities in ppm-meters over the region depicted in Figure 4. In general, the most intense plumes are directly associated with proximity to a dairy farm.

4.2 California Salton Sea

The Salton Sea locale in southern California is a region of considerable geothermal activity that lies at the convergence of the Imperial fault and the southern end of the San Andreas fault. Previous visits to this area with our SEBASS sensor had detected multiple hot spots and several active fumaroles emitting ammonia plumes, believed to result from thermally-induced decomposition of plant matter or other nitrogenous material. Our overflight with the Mako sensor was conducted after sunset, to emphasize the locations of hot spots against the cooling terrain. An example of ammonia detections in this region superimposed on a 53-whisk Mako thermal radiance image is shown in Figure 6.

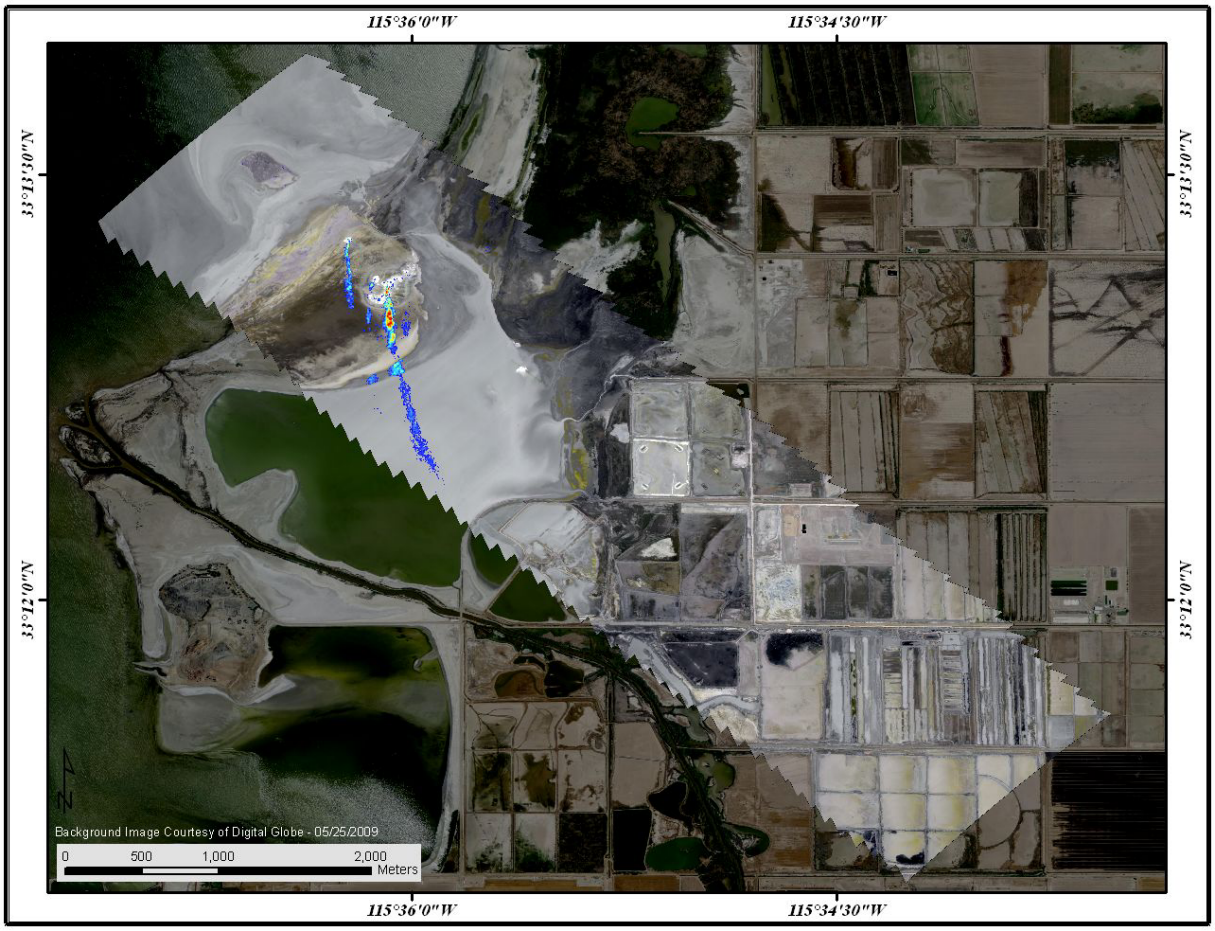

Figure 6. Ammonia plumes (colored lineaments in the upper left quadrant of the image, the longest of which is ~1.5 km in length) at the SE margin of the Salton Sea, as detected with the Mako sensor. The plumes are superimposed on the false color thermal radiance map (using Mako spectral channels at R=11.72, G=10.27, B=8.81 microns). White areas represent hot regions and signify geothermal activity at the surface. These data were acquired from an altitude of 6700 ft. AGL. (Background visible image courtesy of DigitalGlobe.)

5. SUMMARY AND FUTURE PLANS

We have briefly described the successful first flights of the Mako thermal infrared airborne sensor, and the initial analysis of its noise and geolocation performance. Changes to the instrument architecture are in progress that will reduce the sensor noise levels and permit operation at our design FPA frame rate of 2 kHz. The planned improvements are expected to be complete by summer 2011. An additional anticipated enhancement will entail installation of a digital camera to provide visible context imagery. During the next flight series we intend to revisit the field sites described above, and also add study areas that will fully exercise the broad area coverage capability of the instrument.

ACKNOWLEDGEMENTS

This work was funded by the Independent Research and Development program of The Aerospace Corporation. All trademarks, service marks, and trade names are the properties of their respective owners.

REFERENCES

[1] Hackwell, J. A., Warren, D. W., Hansel, S. J., Hayhurst, T. L., Mabry, D. J., Sivjee, M. G., Skinner, J. W., Bongiovi, R. P., "LWIR/MWIR imaging hyperspectral sensor for airborne and ground-based remote sensing," *Proc. SPIE*, **2819**, 102-107 (1996).

[2] Warren, D. W., Boucher, R. H., Gutierrez, D. J., Keim, E. R., Sivjee, M. G., "MAKO: A high performance, airborne imaging spectrometer for the long-wave infrared," *Proc. SPIE*, **7812**, 78120N (2010).

[3] Clarisse, L., Shephard, M. W., Dentener, F., Hurtmans, D., Cady-Pereira, K., Karagulian, F., Van Damme, M., Clerbaux, C., Coheur, P-F., "Satellite monitoring of ammonia: a case study of the San Joaquin Valley," *J. Geophys. Res.*, **115**, D13302 (2010).